Digest Journal of Nanomaterials and Biostructures Vol. 11, No. 1, January - March 2016, p. 123 - 132

THERMAL AND PH SENSITIVE NANO/MICROGELS OF *N*-ISOPROPYLACRYLAMIDE AND CARBOXYALKYL METHACRYLATES

D. A. CASTRO-VIDAL, C. OBESO-VERA, K. A. SUAREZ-MERAZ, B. M. LARA-MOLINERO, A. SERRANO-MEDINA, J. M. CORNEJO-BRAVO*
Universidad Autónoma de Baja California, Facultad de Ciencias Químicas e Ingeniería, Calzada Universidad 14418 Parque Industrial Internacional Tijuana, Tijuana B.C. 22390

We synthesized thermal and pH sensitive nanogels and microgels by a dispersion polymerization method, consisted of *N*-isopropylacrylamide (NIPAAm) and two different carboxyalkyl methacrylates (CAM): 5-methacryloyloxypantenoate potassium salt (M_4K), or 11-methacryloyloxyundecanoate potassium salt ($M_{10}K$). Monodisperse particles were produced with proportions of 5, 10 and 15 mol% of acid comonomers. For the NIPAAm/M_4K copolymers the transition temperature is tuned with the content of the acid monomer; for instance those materials have potential for biomedical applications, such as temperature and/or pH responsive drug delivery. On the other hand, the copolymers with $M_{10}K$ present a size one order of magnitude smaller since the amphiphilic acid monomer acts as a surfactant, however due to the predominantly hydrophobic characteristics of the acid monomer the transition temperature cannot be increased above the temperature of homopolymeric NIPAAm microgels.

(Received November 11, 2015; Accepted January 29, 2016)

Keywords Methacrylates, Dispersion polymerization, Nanogels, *N*-isopropylacrylamide. Dual sensitive polymers.

1. Introduction

Intelligent polymers are soluble, surface-coated or crosslinked polymeric materials capable of undergoing sharp physical or chemical modifications in response to external stimuli such as temperature, pH, ions or other chemical species, electric or magnetic fields [1]. Thermally responsive polymers exhibit a lower critical solution temperature (LCST), below this temperature the polymers are soluble. When temperature rises above the LCST, the polymers undergo a phase transition, collapse and, further, form aggregates. This phenomenon is reversible and thus, when the temperature is lowered, the polymers become soluble again [2]. On the other hand, thermosensitive crosslinked polymers are swollen in water (hydrogel) below a critical transition temperature T_c (related to the LCST). Heating above this transition is followed by spelling of water to the surroundings and shrinkage of the hydrogels. Since this phenomenon is reversible by cooling, these kind of polymeric materials are being studied for their application in drug delivery [3], in separation systems [4,5] and in chemo-mechanical valves [6].

One of the most studied "smart" materials is poly(N-isopropylacrylamide) (PNIPAAm) with a LCST of 32 °C [7]. Based on its LCST so close to the body temperature (37 °C), it is one of the most widely researched thermal sensitive material for biomedical applications, and various nanostructures PNIPAAm materials, including nanogels [8], have been developed as, for instance, drug and gene carriers [9-11], temperature-targeted therapy materials [12-19], and blood-vessel-embolic material [20].

The precise control and tuning of the LCST is a requirement for different applications of these polymeric materials. The LCST can be altered by co-polymerization with hydrophilic or

*Corresponding author: jmcornejo@uabc.edu.mx

hydrophobic monomers [21]. The use of comonomers with ionizable groups, like carboxylic acids or amines, present the advantage over other comonomers that their hydrophobicity/hydrophilicity balance can be modified by changes in the pH of media leading to a pH-tunable LCST [22].

The aim of this work was to develop nano/microgels with a series of NIPAAm-copolymers with tuning capacity for their T_c based on carboxyalkyl methacrylates (CAM) comonomers with hydrophobic spacers and hydrophilic ionizable groups. (Fig. 1). We also study the relationship between the composition and particle size, in a range of temperatures, in pure water and solutions with varying pH.

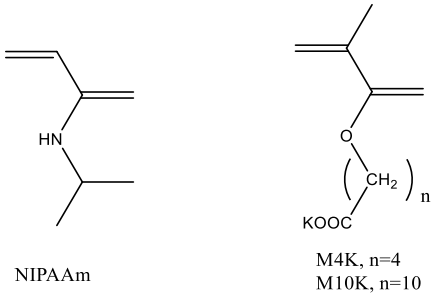

Fig. 1. Chemical structures of NIPAAm, M_4K and $M_{10}K$

2. Experimental

2.1. Materials

NIPAAm (TCI, 98%) was purified by recrystallization in *n*-hexane. Ethylene glycol dimethacrylate (EGDMA) (Aldrich) was purified by passing it through a column of hydroquinone remover from Sigma-Aldrich, ammonium persulfate (APS) (Aldrich, 98%), were used as received. M_4K and $M_{10}K$ were prepared and characterized as previously reported for our group [23-25]. Buffers were prepared at 0.05 M total concentration. The types of buffers used were: pH 3-5, acetate buffers; pH 6 and 7, phosphate buffers; pH 8 and 9 borate buffers; and pH 10, carbonate buffer. Distilled water and buffers were filtered through 0.22 µm filters prior to use to eliminate any particulate matter.

2.2. Synthesis of amphiphilic micro/nanogels particles

The NIPAAm micro/nanogels with different proportions of M_nK copolymers were prepared by dispersion polymerization [26]. The procedure was as follows: 0.5 g of NIPAAm, 0, 5, 10 or 15 mol% of M_4K or $M_{10}K$, 5 mol% of EGDMA, as crosslinker, were dissolved in 50.0 mL of distilled water (Table 1). The solution was stirred for 30 min while being purged with nitrogen to removed oxygen. Afterwards, the solution was heated to 85 $^{\circ}$C in an oil bath for 30 min, and then the initiator (APS 2 mol%) was added to start the reaction. The polymerization process was allowed to continue for 45 min, and stopped by placing the reaction vessel in water/ice bath. The resulting dispersions were purified for 5 days by dialysis using a regenerated cellulose membrane with a 14 kDa molecular weight cutoff (Spectrum Laboratories). Micro and nanoparticles were recovered by freeze drying. The yield was calculated gravimetrically.

2.3. IR spectra

The IR spectra of the samples were recorded by a Fourier transform infrared spectrophotometer (FT-IR, Thermo Scientific Nicolet iS5) by iDS Attenuated total reflectance (ATR) direct method at room temperature using the *OMNIC 9.2.41 software*.

2.4. Particle sizing

The purified (dialyzed and freeze dried) micro/nanogels were resuspended to form a 1 w% in distilled water under magnetic stirring during 2 h minimum and then diluted 10 times with distilled water or different buffers. The size distribution of the samples was evaluated by dynamic

light scattering (DLS) using a Zetasizer Nano NS (DTS 1060; Malvern Instruments, Miami, FL) equipped with a green laser of 532 nm. The angle of the measurement is 173º (backscattering).

2.5. FESEM measurements

Field emission scanning electron microscopy (FESEM) was used to characterize the morphologies of the micro/nanogels. The samples were diluted with isopropyl alcohol, dripped, dried on a silica wafer, and sputter-coated with gold-palladium on a Quorum Sputtering Q150 during 1 min prior to examination on the JEOL equipment.

2.6. Acid content determination

The content of CAM in the nano/microparticles was evaluated by potentiometric acid-base titration. The dried nano/microgel of known weight (0.1g) was immersed in 30 ml of distilled water. Standardized 0.1 M NaOH was added to the nano/microgel dispersion until pH above 11 to ensure complete ionization of the carboxylic acid groups. The dispersions were slowly back titrated with standardized 0.05M HCl solutions until pH 2. The content of carboxyalkyl metacrylate was calculated by the volume of 0.05 M HCl consumed between the inflection points of the titration curve.

2.7. Critical transition temperature evaluation

The effect of the temperature and pH on the particle size of the nano/microgels products was studied by DLS using the same Zetasizer Nano equipment by a temperature trend method edited to go from 20 to 50 ºC every two degrees, equilibrating 4 min once the measurement temperature was achieved. The size distribution reported is the distribution by intensity. The T_c was evaluated as the peaks maxima in the first derivative of the D_h versus temperature. In the case that aggregation occurs, T_c is determined as the temperature where aggregation is measured by DLS.

2.8. Zeta potential

Zeta potential was also measured using the Zetasizer Nano NS by laser Doppler microelectrophoresis. Measurements were performed on folded capillary cells at 25 ^{o}C using the solutions prepared for size determination.

3. Results and discussion

Copolymeric nano/microgels were prepared by a dispersion polymerization method. The reaction is performed above the transition temperature of the materials so that the growing polymer chains form the particulate seeds for the incorporation of the monomers until a nano/microgel is formed. For instance, we used a fix temperature of 85 ºC to intent the production of temperature and pH sensitive nanogels using NIPAAm as the temperature sensitive material and both M_4K or $M_{10}K$ at 5, 10 and 15 mol% (with respect to NIPAAm) as the pH-sensitive molecule. The second number in the nomenclature represents the molar proportion of the ionizable monomer in the feed. Micro/nanogels were synthesized using 2 mol% of an anionic initiator (with respect to NIPAAm), obtaining monomodal size distributions (Fig. 2) [27]. The crosslinker used was EDGMA since good swelling properties have been observed using this crosslinker [28, 29].

Table 1 presents the hydrodynamic diameter (D_h) of the nano/microgel at 25 ^{o}C in water. For the PNIPAAm microgels the size corresponds well with previous reports [28, 29]. The size of the microgels decrease as the proportion of M_4K increases. These results indicate that the amphiphilic acid monomer acts as surfactant in the reaction mixture, decreasing the size of the polymerizing seeds. Particle size is significantly smaller for the copolymers with $M_{10}K$ indicating a stronger surfactant effect for the longer alkyl chain monomer. For the latter case, the size are in the range of the obtained by emulsion polymerization [30]; for instance the reaction can be classified as a soapless emulsion polymerization were the emulsifier is incorporated into the nanogel [31].

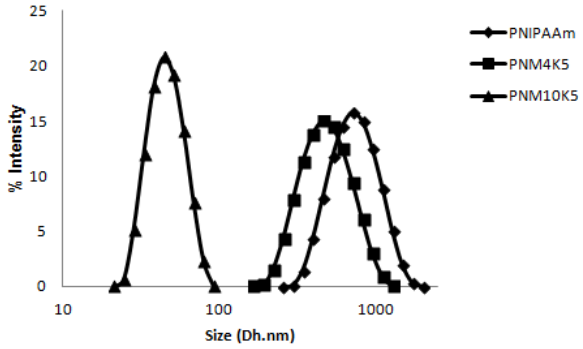

Fig. 2. Size distribution of NIPAAm micro/nanogels in water at 25 ºC, synthesized with 5 mol% of different anionic comonomers (crosslinked with EGDMA 5 mol% and initiated with APS 2 mol%).

Table 1 Synthetic conditions for nano/microgels preparation and its mean average sizes at 25 ºC in water.

Name	Comonomer	Comonomer[a] (mol %)	Yield (weight %)	D_h (nm) (PDI)
PNIPAAm			71	663.9 (0.140)
PNM_4K_5	M_4K	5	80	436.0 (0.120)
PNM_4K_{10}	M_4K	10	86	396.6 (0.267)
PNM_4K_{15}	M_4K	15	86	393.5 (0.201)
$PNM_{10}K_5$	$M_{10}K$	5	70	43.58 (0.054)
$PNM_{10}K_{10}$	$M_{10}K$	10	73	30.50 (0.245)
$PNM_{10}K_{15}$	$M_{10}K$	15	68	27.78 (0.257)

[a] With respect to NIPAAm.

FESEM micrographs of some nano/microgels are presented in Fig. 3. The microscopies corroborate the micro/nanometric dimensions obtained by DLS measurements of the materials synthesized.

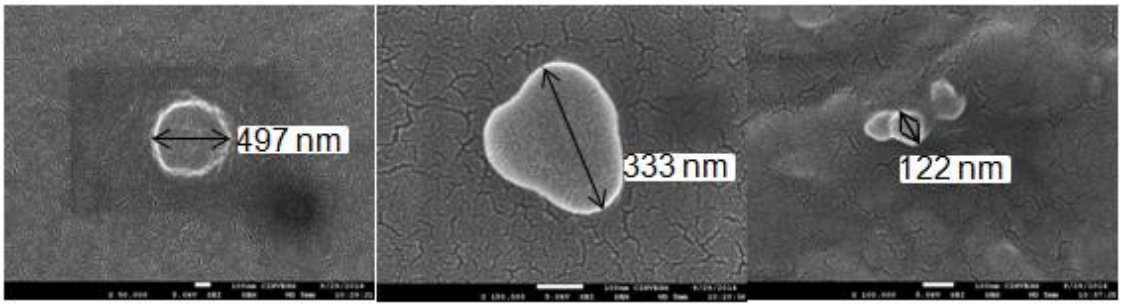

Fig. 3. Topography images of PNIPAAm microgels by FESEM. Left PNIPAAm, center PNM_4K5, right $PNM_{10}K5$.

The FT-IR spectra of PNIPAAm presented in Fig. 4 (a). A broad band appeared between 3600 cm^{-1} (N-H stretching). Peaks at 1635 cm-1 and 1538 cm-1, which is due to the presence of the amide groups (amide band I and II, respectively), and 1385 cm-1 corresponding to the C-H vibrations of $–CH(CH_3)_2$ [32]. A small intensity peak is observed at 1725 cm^{-1} corresponding to the stretching of the carbonyl group of EDGMA.

In Fig. 4 are also shown the FT-IR spectra of PNM_4K_{15} (b) and $PNM_{10}K_{15}$ (c) micro/nanogels. Similar peak are observed for the PNIPAAm microgels except the peak at 1725 cm^{-1} is slightly stronger due to the addition of the signal from the carbonyl on the ester of the

anionic comonomers. The expected peak at 1555 cm^{-1} from carboxylate group [33] is overlapped for the signal from the bending of the amide group.

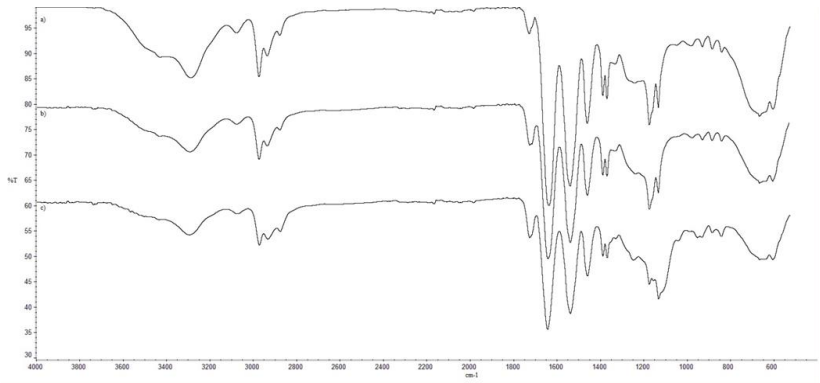

Fig. 4. FT-IR spectra of the PNIPAAm, PNM_4K_{15} and $PNM_{10}K_{15}$.

The content of anionic groups in the hydrogels was determined by acid-base titration is presented in Table 2. An efficient incorporation of the acid groups was observed. Table 2 also present the Z potential of the nano/microparticles in water. More negative values of Z potential are observed as the proportion of acid in the nano/microgels increases.

Table 2. Acid monomer content of nano/microgels and Z potential in deionized water at 25 °C.

Name	Weak acid in feed (weigth%)	Weak acid in nano/microgels (weight%)	Zeta potential at pH 7 (mV)
PNIPAAm			-7.13
PNM_4K5	8.44	7.49	-11.2
PNM_4K10	15.81	14.26	-16.4
PNM_4K15	21.78	22.03	-29.5
$PNM_{10}K5$	10.85	9.56	-7.71
$PNM_{10}K10$	19.41	18.27	-18.8
$PNM_{10}K15$	26.58	25.43	-31.5

Fig. 5 presents the effect on size of the temperature on the different nano/microgels synthetized in water.

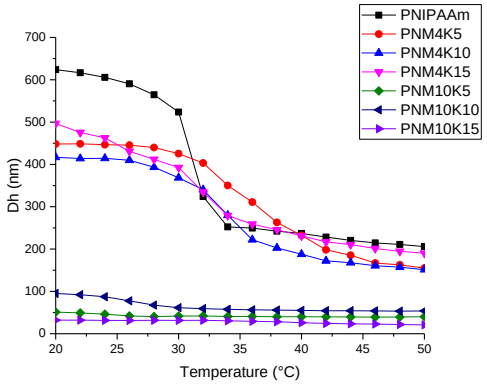

Fig. 5. Effect of temperature in size of nano/microgels in water.

PNIPAAm presents a transition at 32 ^{o}C as reported. On the other hand, the incorporation of M_4K produces a small change on the transition temperature. Table 3 presents the T_c and also the swelling capacity of the different nano/microgels, in water. Swelling capacity was calculated as the ratio $D_{h\ 20\ ^oC}/D_{h\ 50\ ^oC}$, considering that $D_{h\ 50\ ^oC}$ is the hydrodynamic diameter in collapsing limit under the measurement conditions.. The T_c and swelling capacity slightly increases for the microgels containing the comonomer M_4K. It is known that swelling capacity is dependent on rubber elasticity, ionic osmotic and affinity of polymers toward water. These results indicate that the ionic osmotic pressure generated by the carboxylate groups overcame the hydrophobicity generated by the methylene groups in the alkyl side chain of the monomer. The stronger water affinity of the ionic microgels requires a higher temperature to break the hydrogen bonds increasing the T_c. Besides, the copolymers present a broaden temperature transition (continuous transition), which is attributed to inhomogenies produced in the nano/microgels [34]. On the other hand the comonomer $M_{10}K$ shows that the hydrophobicity introduced by the alkyl side chain overcome the ionic osmotic pressure generated by the carboxylate groups, resulting in a decrease on the T_c and on the swelling capacity. For this series of nanogels the size transition with temperature is barely noticeable due to the small void volume available for shrinkage.

Table 3 T_c, Dh of microparticles at 20 and 50 ºC in water, and the swelling ratio ($D_{h\ 20^oC}/D_{h\ 50\ ^oC}$) for the different nano/microgels synthesized.

Name	T_c (ºC)(in water)	D_h nm at 20 ºC (PdI)	D_h nm at 50 ºC (PdI)	$D_{h\ 20^oC}/D_{h\ 50\ ^oC}$
PNIPAAm	32	651.7 (0.075)	252.4 (0.167)	2.58
PNM_4K5	35	446.3 (0.116)	155.5 (0.162)	2.87
PNM_4K10	35	415.8 (0.253)	149.3 (0.397)	2.85
PNM_4K15	34	496.8 (0.194)	190.2 (0.275)	2.61
$PNM_{10}K5$	26	49.85 (0.074)	39.37 (0.033)	1.26
$PNM_{10}K10$	26	92.12 (0.094)	53.98 (0.088)	1.70
$PNM_{10}K15$	26	32.54 (0.047)	24.19 (0.259)	1.34

Fig. 6 present the effect of temperature on size on the pH range from 3 to 10, for the nano/microparticles synthesized. PNIPAAm microgels aggregate at 32 ^{o}C in all media studied, but not in water. It is known that dispersion stability of nanogels produced by the method used here depends upon the repulsion between particles caused by the permanent negative charges generated by the persulfate used as initiator [35]. At the T_c the hydrogen bonds between NIPAAm and water break and the hydrophobic interactions expel water from the microgels. In pure water the microgels shrink since the surface charge is enough to keep the microparticles isolated. However the ionic strength of the buffer solutions used to disperse the nano/microgels screens the charges producing aggregates at the T_c. Aggregation of nanoparticles at the T_c have been observed for copolymers of NIPAAm and allylacetic acid, even at low salt concentration [36].

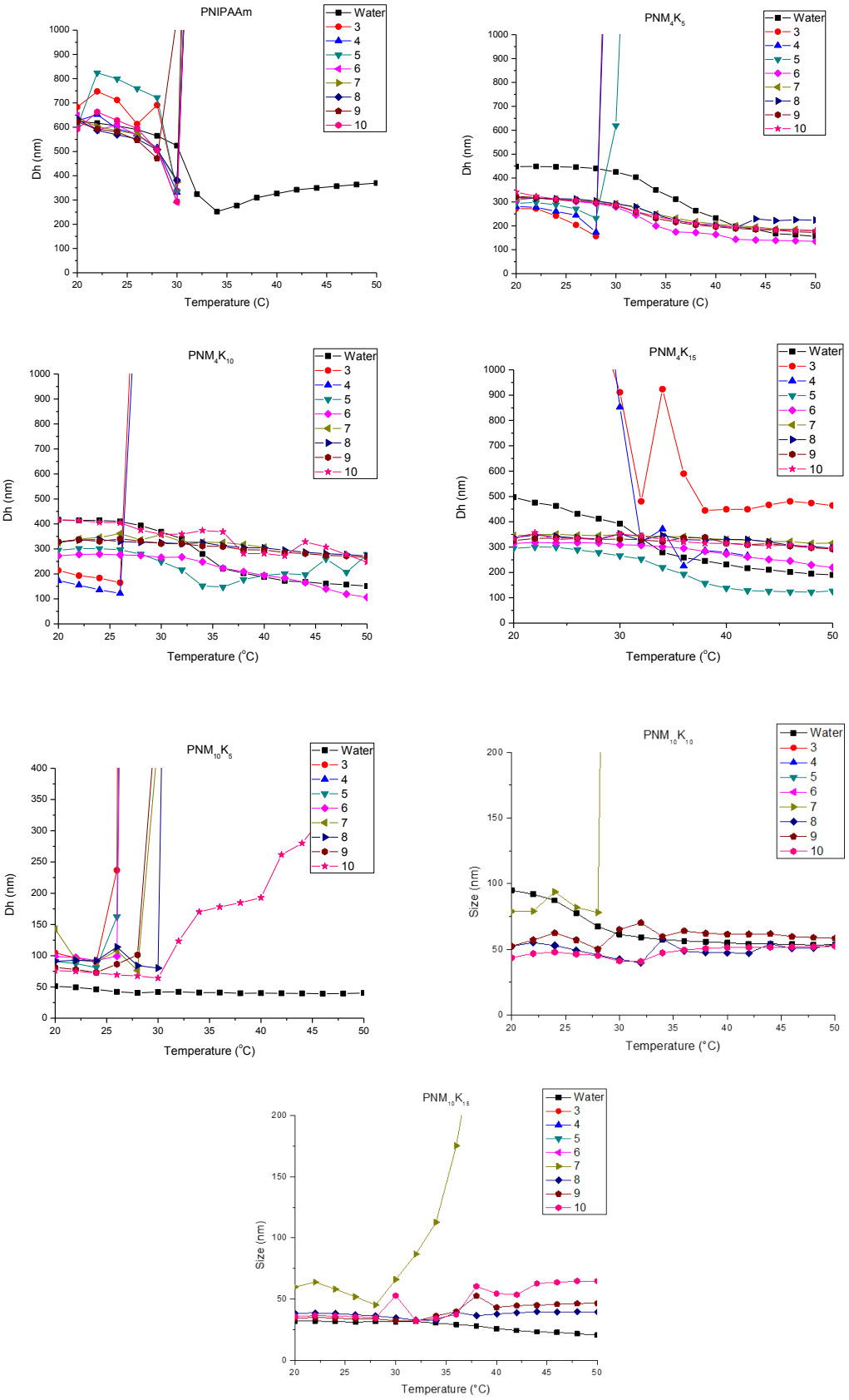

Fig 6. Effect of temperature on size of nano/microgels on the pH range from 3 to 10.

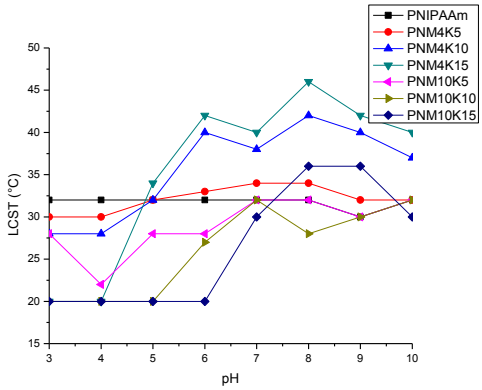

Fig. 7. Effect of pH on the LCST for the different synthetized nano/microgels.

For the copolymers NIPAAm-CAM, there is also stabilization for the charges of the carboxylate groups. However, at low pH the carboxylic acid groups are unionized, decreasing hydrogen bonding with water; while the hydrophobic character of the aliphatic side chains produces a decrease on the Tc. For the microgels PNM_4K_5 aggregation occurs at pH 3 to 5. At these pH values the acid monomer is in the unionized form since the measured pK_a for the M_4K homopolymer is 6.14 [25], for instance at pH 5 less of 10% of the carboxylic acid groups are ionized. For the copolymer PNM_4K_{10} and PMN_4K_{15}, aggregation occurs only at pH 3 and 4. Figure 7 presents the T_c at different pH values. The T_c increases for the copolymers of M_4K as the pH increases due to increase on the ionization of the nanoparticles, making the material more hydrophilic. However at pH 9 and 10 the T_c is below the T_c at pH 8. At higher pH the concentration of Na^+ in the media increases producing charge screening and decreasing the effect of charges on swelling [37]. A result to pinpoint is that at pH 7, the T_c increases as the content of M_4K increases, reaching values above the normal body temperature, which could be important for biomedical applications.

For the nanogels $PMN_{10}K_5$ aggregations occurs in all cases, except in water. The aggregation point is below the T_c of PNIPAAm and decreases at the pH decreases. The longer aliphatic side chain of the comonomer $M_{10}K$ generates stronger hydrophobic interactions decreasing the Tc. Besides, the hydrophobic microenvironment produced by the side chains increases the pK_a of the weak acid, been 7.4 for the homopolymer $M_{10}K$ [38], requiring a higher pH for ionization of the carboxylic acid groups. For the nanogels $PNM_{10}K_{10}$ and $PNM_{10}K_{15}$ aggregation occurs up to pH 7. Some lines are not observed in Figure 6, especially at low pH values, because aggregation occurs even at 20 °C, the lowest temperature evaluated. For those cases Tc was considered 20 ^oC in Figure 7.

The results correlate well with a study of the linear copolymers of NIPAAm-CAM: copolymerization of NIPAAm with M_4K produces a slight increase on the LCST (measured as the point of precipitation) at pH values above the pKa of M_4K, but LCST decreases for copolymers with $M_{10}K$, at any pH [38]. Decrease on Tc was attributed to the formation of hydrogen bonds between the carboxylate groups and the amide groups of NIPAAm decreasing the interaction of the polymers with water leading to lower solubility and decrease on the LCST. The result also correlates with the results for copolymeric hydrogels of NIPAAm-CAM. In that case, T_c measured as the maximum on the decrease on diameter of discs [39] or rods [40].

4. Conclusions

Herein, we reported the synthesis and characterization of monodisperse “smart” micro/nanogels that exhibit a volume phase transition at physiologically relevant temperatures and pH values.

With the copolymerization of NIPAAm and acidic monomers derivative from carboxylic acids, it was possible to obtain copolymeric nano/microgels.

The monomer used has a significative effect on size and pH sensitivity of the nano/microgels. Copolymerization with M_4K produces microgels with smaller size than PNIPAAm microgels. These materials are temperature and pH sensitive. The T_c can be tuned with the proportion of acid monomer used; for instance the materials have great potential for biomedical applications (e.g. temperature and/or pH triggered drug delivery).

On the other hand copolymerization of NIPAAm with an acid comonomer, containing ten methylenes aliphatic spacer, produces particles of considerably smaller size, indicating that the monomer acts as a stabilizer during nanoparticle synthesis. Due to the hydrophobic effect of the aliphatic side chains aggregation of the particles is observed at temperatures below the T_c of PNIPAAm microgels.

The method used here is a facile and fast alternative to produce nanometric polymeric materials without the need of using solvents, as in the inverse emulsion polymerization method; or high amounts of surfactants, which are difficult to eliminate, as in both inverse and normal emulsion polymerization methods.

Our study shows that these gels can be tailored for the required application, tuning the size and the specific transition temperature as a function of type and proportion of CAM.

Acknowledgments

Work supported by SEP-CONACYT (CB2010-1-157173). DACV thanks Scholarship No. 318269 by CONACYT and grant from UABC. The authors thank Ana Ruth Cristobal, Dora A. Huerta Q. and Patricia Quintana from Centro de Investigación y Estudios Avanzados Unidad Mérida for FESEM images. JMCB thanks CONACYT for Abroad Sabbatical Stay fellowship (232833).

References

[1] F. Bignotti, M. Penco, L. Sartorea, I. Peroni, R. Mendichi, M. Casolaro, A. D'Amore, Polymer **41**, 8247 (2000).
[2] H.Vihola, A. Laukkanen, L. Valtola, H. Tenhu, J. Hirvonen, Biomaterials **26**, 3055 (2005).
[3] T. Okano, A. Kikuchia, Y. Sakuraia, Y. Takeib, N. Ogatab, J. Control. Release **36**, 125 (1995).
[4] R. Freitas, E. Cussler, Chem. Eng. Sci. **42**, 97 (1987).
[5] E. Vasheghani-Farahani, D. Cooper, J. Vera, M. Weber, Chem. Eng. Sci. **47**, 31 (1992).
[6] K. Arndt, D. Kuckling, A. Ritchter, Polym. Adv. Technol. **11**, 496 (2000).
[7] D. A. Ossipov, S. Piskounova, J. Hilborn, Macromolecules **41**, 3971 (2008).
[8] N. Morimoto, T. Ohki, K. Kurita, K. Akiyoshi, Macromol. Rapid Commun. **51**, 672 (2008).
[9] W. H. Blackburn, E. B. Dickerson, M. H. Smith, J. F. McDonald, L. A. Lyon, Bioconjugate Chem. **20**, 960 (2009).
[10] Y. M. Zhoua, A. Ishikawaa, R. Okahashia, K. Uchidac, Y. Nemotoa, M. Nakayamaa, Y. Nakayamaa, J. Control. Release **123**, 239 (2007).
[11] B. R. Twaites, C. Heras-Alarcón, M. Lavigne, A. Saulnier, S. S. Pennadam, D. Cunliffe, D. C. Górecki, C. Alexander. J. Control. Release **108**, 472 (2005).
[12] A. Aqil, S. Vasseur, E. Duguet, C. Passirani, J. P. Benoit, R. Jérome, C. Jérome, J. Mater. Sci. **18**, 3360 (2008).
[13] J. K. Oh , R. Drumright, K. Matyjaszewski, Prog. Polym. Sci. **33**, 448 (2008).
[14] M. Ballauff, Y. Lu, Polymer **48**, 1815 (2007).
[15] C. Lin, W. Y. Chiu, Polymer **46**, 10092 (2005).
[16] W. Leobandung, H. Ichikawa, Y. Fukumori, N. A. Peppas, J. Control. Release **80**, 357 (2002).
[17] W. Leobandung, H. Ichikawa, Y. Fukumori, N. A. Peppas, J. Appl. Polym. Sci. **80**, 1678 (2003).
[18] J. Alvarez-Sánchez, A. Licea-Claveríe, J. M. Cornejo-Bravo, C. W. Frank, React. Funct.

Polym. **71**, 1077 (2009).
[19] T. Hoare, R. Pelton, Biomacromolecules **9**, 733 (2008).
[20] X. Li, W. Liu, G. Ye, B. Zhang, D. Zhu, K. Z Yao, Z. Liu, X. Sheng, Biomaterials **26**, 7002 (2005).
[21] H. Feil, Y. H. Bae, J. Feijen, S. W. Kim, Macromolecules **26**, 2496 (1993).
[22] G. Chen, A. S. Hoffman, Macromol. Chem. Phys. **196**, 1251 (1995).
[23] E. Rogel-Hernández, A. Licea-Claveríe, J. M. Cornejo-Bravo, K. F. Arndt, Des. Monom. Polym. **4**, 343 (2001).
[24] A. Licea-Claveríe, E. Rogel-Hernández, R. Salgado-Rodríguez, J. A. López-Sánchez, L. A. Castillo, J. M. Cornejo-Bravo, K. F. Arndt, Macromol. Symp. **207**, 193 (2004).
[25] J. M. Cornejo-Bravo, J. E. Vazquez-Altamirano, E. Rogel-Hernandez, A. Licea-Claverie. M. A. Ramos-Ibarra, Des. Mon. Polym. **10**, 271 (2007).
[26] J. K. Oh, R. Drumright, D. J. Siegwart, K. Matyjaszewski, Prog. Polym. Sci. **33**, 448 (2008).
[27] M. Gaumet, A. Vargas , R. Gurny , F. Delie, Eur. J. Pharm. Biophar. **69**, 1 (2008).
[28] A. Serrano-Medina, J. M.Cornejo-Bravo, A. Licea-Cleveríe, J. Colloid Interface Sci. **369**, 82 (2012).
[29] C. Obeso-Vera, J. M. Cornejo-Bravo, A. Serrano-Medina, A. Licea-Claverie, Polym. Bull. **70**, 653 (2012).
[30] S. Zhou, B. Chu, J. Phys. Chem. B **102**, 1364 (1998).
[31] B. R. Saunders, B. Vincent, Adv. Colloid Interface Sci. **80**, 1 (1999).
[32] N. Seddiki, D. Aliouche , Bull. Chem. Soc. Ethiop. **27**, 447 (2013).
[33] J. M. Cornejo-Bravo, M. E. Flores-Guillen, E. Lugo-Medina, A. Licea-Claverie, Int. J. Pharm. **305**, 52 (2005).
[34] S. Zhou, B. Chu, J. Phys. Chem. B **102**, 1364 (1998).
[35] R. Arshady, Colloid Polym. Sci. **270**, 717 (1992)
[36] M. Karg, I. Pastoriza-Santos, B. Rodriguez-Gonzalez, R. Von Klitzing, S. Wellert, T. Hellwert, Langmuir **24**, 6300 (2008).
[37] T. Wan, Q. Chen, Q. Zhao, R. Huang, L. Liao, J. Xiong, L. Tang, J. Appl. Polym. Sci. **132**, 42139 (2015).
[38] R. Salgado-Rodríguez, A. Licea-Claveríe, K.F. Arndt, Eur. Polym. J. **40**, 1931 (2004).
[39] A. Licea-Claverie, J. M. Cornejo-Bravo, R. Salgado-Rodriguez, D. R. Santos-Rosas, E. Lugo-Medina, M. A. Ramos-Ibarra, K. F. Arndt, Macromol. Symp. **254**, 292 (2007).
[40] R. Salgado-Rodríguez, A. Licea-Claverie, A. Zizumbo-López, K. F. Arndt, J. Mex. Chem. Soc. **57**. 118 (2013).